

# Estimation of Ground Motion Variability in the CEUS Using Simulations

Xiaodan Sun

Associate Professor, Southwest Jiaotong University, Chengdu, China

Sanaz Rezaeian,

Research Structural Engineer, U.S. Geological Survey (USGS), Golden, CO, USA

Brandon S. Clayton

Geophysicist, U.S. Geological Survey (USGS), Golden, CO, USA

Stephen Hartzell

Geophysicist, U.S. Geological Survey (USGS), Golden, CO, USA

**ABSTRACT:** We estimate earthquake ground-motion variability in the central and eastern U.S. (CEUS) by varying the model parameters of a deterministic physics-based and a stochastic site-based simulation method. Utilizing a moderate-magnitude database of recordings, we simulate ground motions for larger-magnitude scenarios M6.0, 6.5, 7.0, 7.5, and 8.0. For the physics-based method, we vary the faulting mechanism, slip, stress drop, rupture velocity, source depth, and 1D velocity structure. For the stochastic method, we simulate realizations using a set of six model parameters, each of which has a preassigned probability distribution. The median spectral accelerations over all synthetic realizations are compared with the NGA-East models. The synthetic standard deviation for deterministic simulations ranges from approximately 0.4 to 0.85 for various magnitudes and distances, whereas that for stochastic simulations is between 0.48 and 1.04. Based on the simulation results and comparisons with NGA-East variability models, a range for ground motion variability in the CEUS is discussed.

## 1. INTRODUCTION

Estimation of ground-motion variability is a fundamental step in probabilistic seismic hazard analysis (PSHA). However, compared to crustal earthquakes in tectonically active regions of the western U.S. (WUS), research on ground-motion variability in stable continental regions of the central and eastern U.S. (CEUS) is lagging due to the lack of ground motion recordings. Most of the variability studies in the CEUS are associated with the development of a new ground motion prediction equation, GMPE (Silva *et al.*, 2002; Atkinson and Boore, 2006). Some variability models for this region have been developed from those based on WUS (Campbell, 2003; Tavakoli and Pezeshk, 2005; Pezeshk *et al.*, 2011). More recently, simulations have been utilized together with the limited number of recordings to better

investigate the ground-motion variability (Imtiaz *et al.*, 2015; Vyas *et al.*, 2016; Crempien and Archuleta, 2017; D'Amico *et al.*, 2017; Frankel *et al.*, 2018). In our previous work (Sun *et al.*, 2015; Rezaeian *et al.*, 2017), we modeled the 2011 M5.8 Mineral, Virginia, earthquake and the 2001 M7.6 Bhuj, India, earthquake, the latter considered a tectonic analog for a large-magnitude CEUS event. We used two different ground-motion simulation methods: a deterministic physics-based (Hartzell *et al.*, 2005) and a stochastic site-based method (Rezaeian and Der Kiureghian, 2010). Both models showed a good fit to the Mineral and Bhuj observations in terms of the median spectral accelerations for a wide range of frequencies (0.1 to 10 Hz). We also simulated ground motions for M5.8, 6.5, 7.0, and 7.6

scenarios in the CEUS, using the two models and made comparisons with existing GMPEs in the CEUS. Both models were shown to be plausible alternatives to predict large-magnitude ground motions in the CEUS. These two models are very different, but complementary to each other, yielding a broader perspective on epistemic ground-motion uncertainties. Therefore, in this work, we utilize the same two approaches to simulate ground motions and quantify their aleatory variabilities (i.e., sigma) for earthquake scenarios **M**6.0, 6.5, 7.0, 7.5, and 8.0. We will compare these variabilities to the sigma models from existing GMPEs and to the new developed model from NGA-East for U.S. Geological Survey (USGS).

## 2. CEUS SIMULATION METHODOLOGY

As previously mentioned, we use two different simulation methodologies. In general, physics-based models are known to produce realistic waveforms at long spectral periods (about  $>1$  s), but they are computationally intensive and require a thorough knowledge of the seismic environment for their source and material models. Stochastic models, on the other hand, may be less accurate in representing the long-period character of actual recordings, but are computationally tractable and incorporate what is known about ground motion source, path, and site characteristics into simple functional forms.

### 2.1. Deterministic physics-based approach

The deterministic physics-based approach in this study (Hartzell *et al.*, 2005) has a kinematic rupture model for the earthquake source. To quantify the ground motion variability, we vary the fault mechanism, slip, stress drop, rupture velocity, source depth, and the 1D velocity structure. The variation of the model parameters are listed in Tables 1 and 2 (see Sun *et al.*, 2018, for parameter definitions).

For the material model, two different 1D velocity models, MIN15 and MIN16, are considered. These velocity models are modified from ones proposed by Saikia (1994) for the eastern United States such that they have a hard

rock surface shear-wave velocity of 3000 m/s, consistent with the work of Pacific Earthquake Engineering Research Center (PEER) in the CEUS (Goulet *et al.*, 2017). They represent two approximate end members: MIN16, with simple increasing velocities with depth, and MIN15, with alternating layers of high and low velocities to better simulate the propagation of  $L_g$  waves. The  $Q$  model, describing the anelastic attenuation, does not vary.

Table 1 Magnitude-independent Parameters Used in Physics-Based Models

Strike (°)	Dip (°)	Rake (°)	Rupture Velocity (km/s)	Rupture Mode	Velocity Model
29	45	0	2.5	Unilateral	MIN15
—	90	45	2.8	Bilateral	MIN16
—	—	90	3	—	—

Table 2 Magnitude-dependent Parameters Used in Physics-Based Models

	$f_0$ (Hz)		$\gamma$		$Z_{top}$ (km)		$L$ (km)	$W$ (km)	$D$ (km)		
<b>M</b> 6.0	6.5	8.5	11	13	2	2.5	4	7	7	6	8
<b>M</b> 6.5	6.5	8	8	10	2	2.5	4	13	10	6	8
<b>M</b> 7.0	3.5	5	4.5	6	1	2	3	25	15	10	8
<b>M</b> 7.5	3.5	5	3.5	5	1	2	3	70	20	10	15
<b>M</b> 8.0	5	6	3	4.5	1	—	—	150	35	10	15

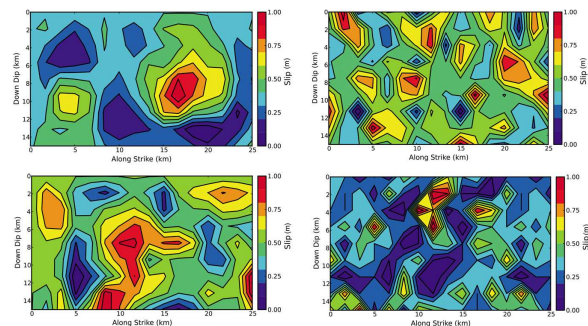


Figure 1: Slip distributions used for the **M**7.0 source.

For each magnitude, four different random slip distributions are considered with wavenumber spectral falloff of  $k^{-2}$ , where  $k$  is the wavenumber. A range of slip correlation lengths is used that is consistent with slip distributions found from source inversions, which yield

different distributions of higher and lower stress drops over the rupture surface. Figure 1 shows the four slip distributions for the **M7.0** scenario, with different correlation lengths along strike and dip.

## 2.2. Stochastic site-based approach

The site-based stochastic model (Rezaeian and Der Kiureghian, 2010) uses a stochastic process to describe the ground motion time-series; it implicitly accounts for the effects of source, path and site conditions through the model parameters. These model parameters are fitted to recorded motions with known earthquake and site characteristics and include the Arias intensity,  $I_a$ , duration of motion,  $D_{5-95}$ , and time at the middle of strong shaking phase,  $t_{mid}$  (which together control the evolving intensity of the motion), and the predominant frequency,  $\omega_{mid}$ , its rate of change with time,  $\omega'$ , and the bandwidth,  $\zeta$  (both of which control the frequency content of the motion). We assigned probability distributions to each parameter, using different databases of recorded motions; Figure 2 shows these distributions for the WUS, CEUS moderate-magnitude events, and Mineral **M5.8** recordings.

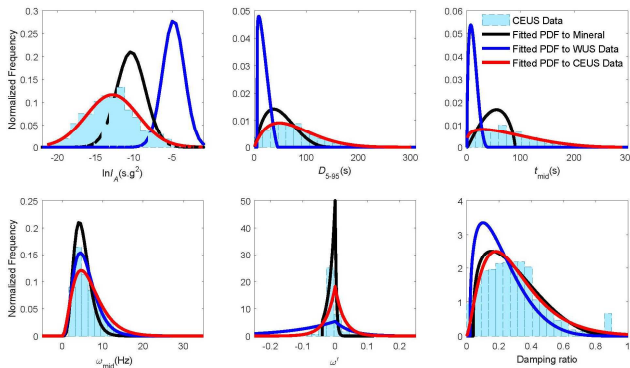


Figure 2: Distributions of the model parameters.

To simulate ground motions for a scenario earthquake in the CEUS with a magnitude larger than 6.0, we developed a model based on the data from the **M5.8** Mineral earthquake and magnitude scaling factors using the Bhuj **M7.6** earthquake (Rezaeian *et al.*, 2017). The magnitude scaling factors are for adjusting each parameter from a **M5.8** to a **M7.6**. Linear interpolation is used for in-between magnitudes and is shown to generate

reasonable results in Rezaeian *et al.* (2017) based on comparisons with existing GMPEs. We use this model (i.e., Mineral-Bhuj) to simulate ground motions for each magnitude scenario at 20 distances uniformly distributed on a log-scale from 10 to 800 km. The  $V_{S30}$  is taken as the largest  $V_{S30}$  in the database, which is 1130 m/s for the Mineral-Bhuj simulations, to be comparable to the recently developed NGA-East GMPEs with a reference-rock condition of  $V_{S30} = 3000$  m/s (Goulet *et al.*, 2017). At each distance, 50 realizations of randomly orientated ground motion components are generated.

## 3. SIMULATION RESULTS

### 3.1. Deterministic physics-based simulations

Using the parameters in Tables 1 and 2, we simulate ground motions for each magnitude scenario at several hundred stations around the fault. All the combinations of the model parameters lead to 6912 scenarios for **M6.0**, 6.5, 7.0, and 7.5, and 2304 scenarios for **M8.0**. For each simulation, the ‘‘average’’ horizontal motion, RotD50, is calculated for eight periods (0, 0.2, 1.0, 2.0, 3.0, 5.0, 7.5, and 10 s). These values are then compared with the 17 GMPEs of the NGA-East for the USGS model (Goulet *et al.*, 2017), and the 2014 USGS-weighted combination of older GMPEs (Petersen *et al.*, 2014). An example comparison for 0.2 and 1.0 s for **M7.0** scenario is shown in Figure 3. Similar figures for other magnitudes and periods are not presented here.

From Figure 3 and the results for other magnitudes, we can see that the reference GMPEs are within the range of the realizations, indicating that the physics-based synthetics are capable of representing the ground motion intensities predicted by other GMPEs. In addition, the median over all realizations is relatively centered within the range of values predicted by the 17 GMPEs of the NGA-East for the USGS model. The median of the synthetics is also close to the 2014 USGS GMPE in terms of amplitude and attenuation at most periods and distances. For larger magnitudes (**M7.5** and 8.0), the synthetic median is slightly higher than the 2014 USGS

GMPE at medium periods ( $1 \text{ s} \leq T \leq 2 \text{ s}$ ). This may be attributed to the fact that most records used in calibrating the model parameters are from moderate magnitude events.

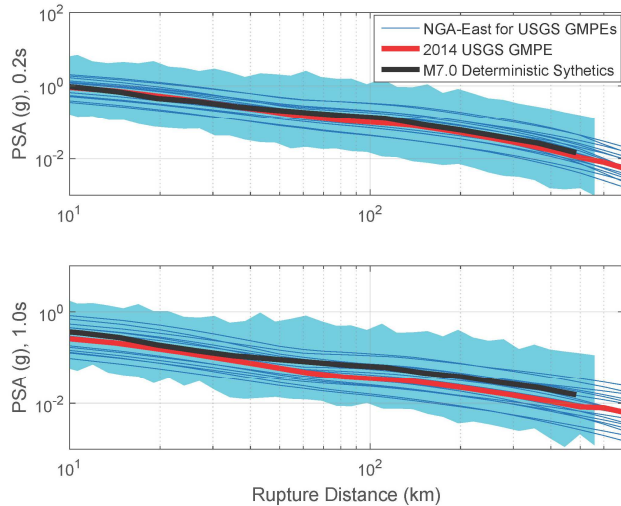


Figure 3: Synthetic RotD50 ground motions at 0.2 and 1.0s (light blue shaded area) for M7.0 scenario, using deterministic physics-based approach. The median over all realizations is plotted in black line. The existing GMPEs are superimposed for reference.

### 3.2. Stochastic site-based simulations

The simulated spectral accelerations—using the stochastic Mineral-Bhuj model with the example of the M7.0 scenario—are shown in Figure 4 for 0.2 and 1.0 s spectral periods. The envelope of the spectral values is plotted as a yellow shaded region, the median over all realizations is a black line. The blue curves represent the 17 GMPEs of the NGA-East for the USGS model, and the red curve represents the 2014 USGS GMPE.

Figure 4 and other similar figures for different magnitudes and periods show the capability of the stochastic synthetics to represent the possible ground motions predicted by GMPEs (i.e., GMPEs are generally within the range of the simulations except at large distances). Similar to the results from the deterministic approach, the median over all realizations is relatively centered within the range of values predicted by the NGA-East for USGS GMPEs for most periods at distance shorter than 100 km and is close to the 2014 USGS GMPE in terms of amplitude and

drop off with distance. As period increases, the attenuation of the synthetics with distance becomes faster than that of the GMPEs. This results in a lower estimation at distances greater than 200 km. This faster attenuation is also reported in Rezaeian *et al.* (2017) when simulating magnitude scenarios between M5.8 and 7.6. Recall that the stochastic approach is record based; therefore, the behavior of the synthetics reflects the behavior of the observed data. In this study, the data used to calibrate the parameters of the stochastic model are from the Mineral and Bhuj earthquakes, both of which also suggest a faster attenuation with distance than existing GMPEs (Figures 15 and 16 in Rezaeian *et al.*, 2017).

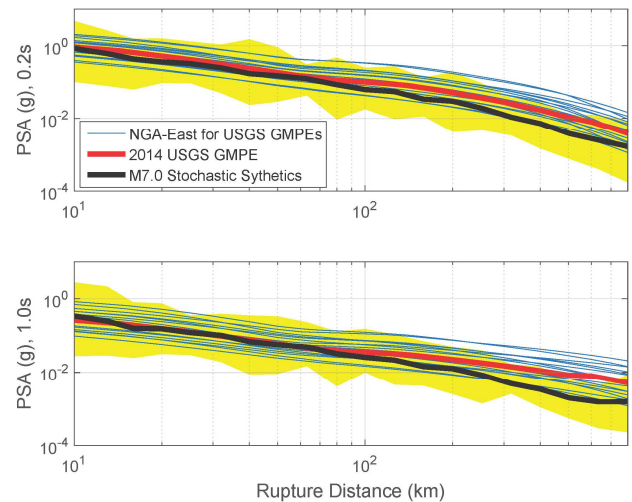


Figure 4: Synthetic RotD50 ground motions at 0.2 and 1.0s (yellow shaded area) for M7.0 scenario, using stochastic approach based on the Mineral-Bhuj model. The median over all realizations is plotted in black line. The existing GMPEs are superimposed for reference.

## 4. VARIABILITY OF SYNTHETICS

Sigma of the synthetics (i.e., standard deviation of natural logarithm of the RotD50 spectral values) is calculated. For the deterministic simulation, the sigma ranges from approximately 0.4 to 0.85 natural log units for various magnitudes and distances, whereas that of the stochastic Mineral-Bhuj simulation is between 0.48 and 1.04 natural log units. Synthetic sigma is plotted versus distance for all magnitudes and

periods. Due to space limitation, only sigma plots for **M6.0** and **7.0** scenarios are shown below in Figures 5 (for deterministic simulations) and 6 (for stochastic simulations).

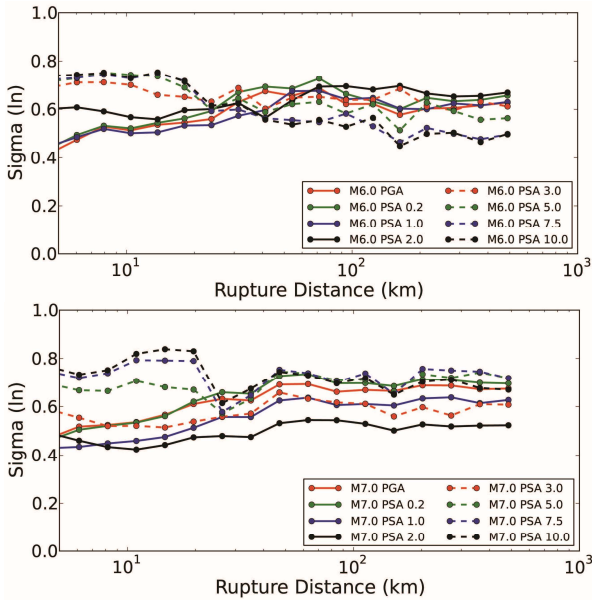


Figure 5: Synthetic sigma versus rupture distance for different periods for **M6.0** and **7.0** scenarios obtained by using the deterministic physics-based approach.

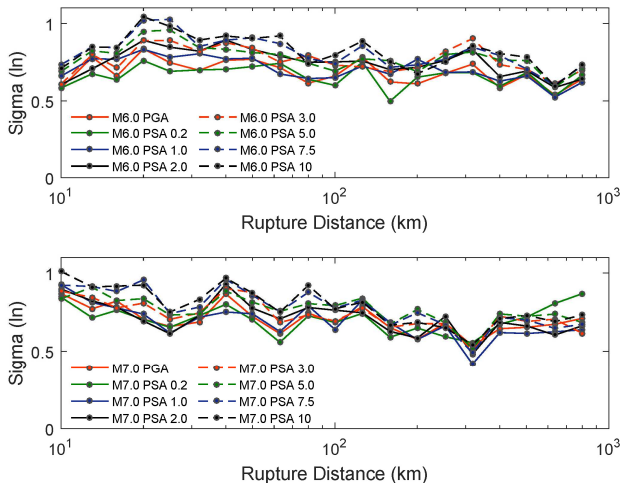


Figure 6: Synthetic sigma versus rupture distance for different periods for **M6.0** and **7.0** scenarios obtained by using the stochastic site-based approach.

Figure 6 indicates that, in the stochastic simulations, there is no systematic dependence of sigma on distance and no trend of sigma, increasing or decreasing, with period. The difference among sigmas for different periods is not large. By contrast, in the deterministic simulations (Figure 5), a slight increase of sigma with distance for short periods ( $T < 2$  s) can be observed. A trend can be observed from both Figures 5 and 6 that, at distances shorter than 100 km, the sigma for long periods ( $T > 3$  s) are always larger than that for short periods. This trend is obvious in the deterministic simulations within 30 km. This is consistent with the findings of Moschetti *et al.* (2017) and Frankel *et al.* (2018) that longer-period variability is more sensitive to variations in near-field rupture directivity than short-period ground motion. However, for **M7.5** and **8.0** deterministic scenarios (not shown), the higher sigma values for longer periods at closer sites are not observed. Particularly, for **M8.0** at long periods ( $T = 7.5$  and  $10$  s), sigma shows an increase (about 0.1) within the distance range of about 15-150 km. The different behavior at larger magnitudes may indicate the need of deterministic simulations for more stations to properly sample rupture directivity effects.

Sigmas for all magnitudes are shown together in Figures 7 (deterministic approach) and 8 (stochastic approach) for 0.2 and 1.0 s. It is difficult to see any obvious variation in sigma with magnitude. Increasing sigma with decreasing magnitude reported by D'Amico *et al.* (2017) is not clearly seen. For the deterministic results, the difference among the sigmas for different magnitudes slightly increases as the period changes from 0.2 to 1.0 s, which is not clearly shown in the stochastic results. Note that, the synthetic sigma of the stochastic modeling comes from three sources: the sigma of the white-noise process, the sigma of the PDF of the model parameters, and the sigma of the predictive equations from regression on each parameter—none of which are dependent on magnitude or distance. Therefore, the total sigma of the synthetics is magnitude- and distance-

independent in this model. If more data become available in the future and support a strong dependence of sigma on these parameters, the stochastic model could be adjusted.

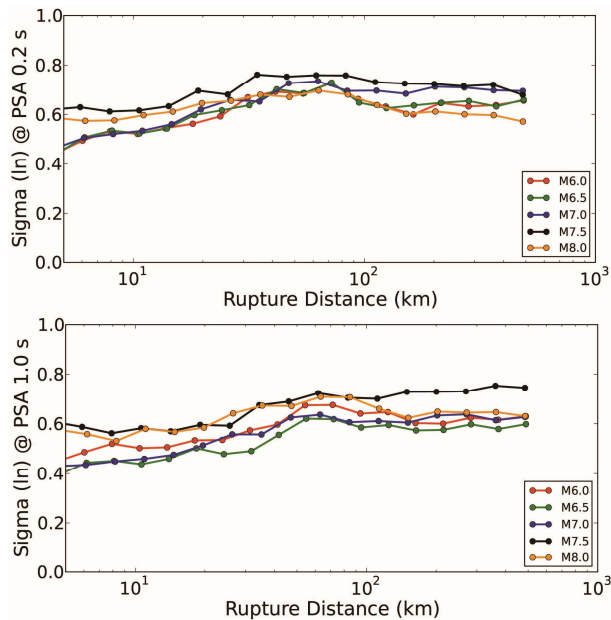


Figure 7: Synthetic sigma versus rupture distance for all magnitudes for PSA at 0.2 and 1.0 s obtained by using deterministic approach.

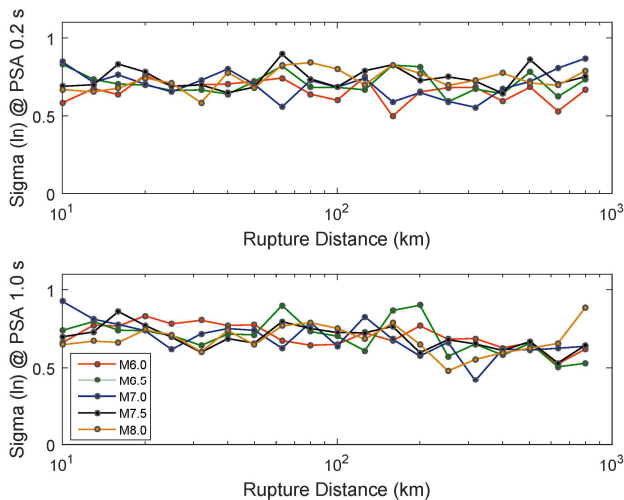


Figure 8: Synthetic sigma versus rupture distance for all magnitudes for PSA at 0.2 and 1.0 s obtained by using stochastic approach.

In Figures 9 and 10, the resulting synthetic sigmas (i.e., aleatory variability of ground

motions) are compared with GMPE estimates from the NGA-East for the USGS model, and the GMPEs used in the 2014 USGS model, for 0.2 and 1.0 s examples, and the two magnitude scenarios M6.0 and 7.0.

In these figures, the light blue curves give estimates of sigma from the nine GMPEs used in the 2014 USGS model (Petersen *et al.*, 2014), which range from 0.41 to 1.01 in natural log units for various magnitudes, distances, and periods. The black curves are the estimates of sigma from the NGA-East for the USGS model (Goulet *et al.*, 2017), which were based mainly on WUS data because of the difficulties that exist in obtaining an independent sigma estimate for the CEUS due to lack of sufficient data for large-magnitude events. The blue and red curves represent the synthetic sigma from using our stochastic site-based approach and our deterministic physics-based approach, respectively.

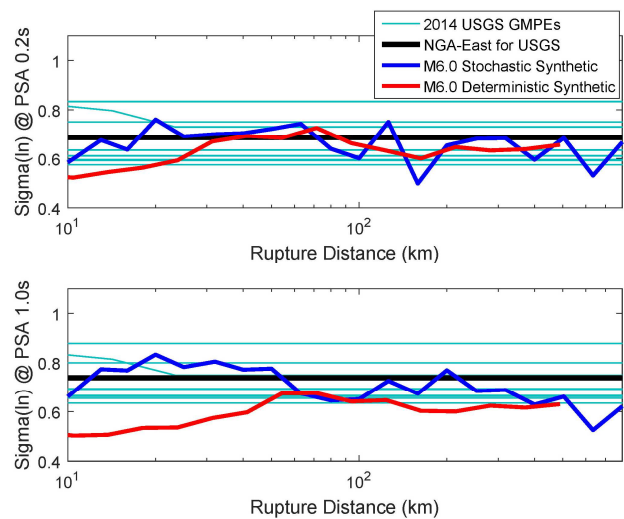


Figure 9: Synthetic sigma over all realizations, compared to the estimates of sigma from the NGA-East for the USGS model (black line), and from the GMPEs used in the 2014 USGS model (light blue lines) for the M6.0 scenario.

Figures 9 and 10 indicate that the range of sigmas from the nine GMPEs used in the 2014 USGS model contains the sigma estimates from our simulations for all magnitudes and for most distances. A commonly occurring dip towards

lower values is seen in the sigma of the deterministic physics-based simulations at short periods close to the fault (less than 30 km, and  $T \leq 1$  s). This lower sigma may be due to the limited number of slip realizations used in the deterministic simulations. Greater variability in slip will produce greater variability in ground motion primarily for stations close to the fault, with a reduced effect at greater distances.

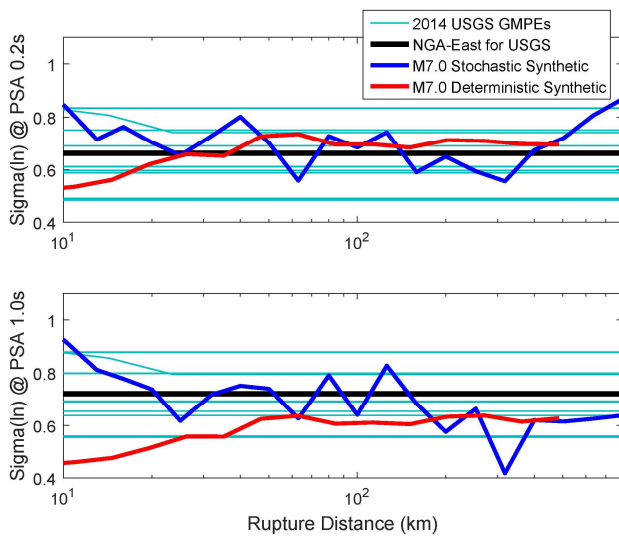


Figure 10: Synthetic sigma over all realizations, compared to the estimates of sigma from the NGA-East for the USGS model (black line), and from the GMPEs used in the 2014 USGS model (light blue lines) for the M7.0 scenario.

The sigmas of the stochastic simulations are in general comparable to the estimates of the NGA-East for the USGS model for most periods (not all periods are shown here), and for all magnitudes and distances. The same is true for the sigmas of the deterministic simulations for 0.2 s. For 1.0 s spectral period, the sigma of deterministic simulations is systematically lower. This agrees with the findings of Al Atik (2015) that the global  $\sigma$  model for the CEUS is lower than the WUS models in this period range.

## 5. PROPOSED SIGMA RANGE FOR CEUS

Based on our estimates of the aleatory variability (i.e., sigmas) from the two simulation approaches, we propose a range of sigma for the

CEUS. We first calculate the range of sigma for each simulation approach based on the fluctuation with distance. According to Keefer and Bodily (1983), we assume the uncertainty of the ground-motion variability follows a  $\chi$ -square distribution. Then, we calculate the median, high, and low estimates for sigmas of  $T \leq 1$  s and  $T > 1$  s by the 5<sup>th</sup>, 50<sup>th</sup>, and 95<sup>th</sup> percentiles of the continuous scaled  $\chi$ -square distribution, respectively, as listed in Table 3. Based on Table 3, we propose a range of sigma for the CEUS which uses the lower estimate of sigma from the physics-based approach as the lower bound, and the higher estimate of sigma from the stochastic approach as the upper bound. This gives a sigma range of 0.45 to 0.83 natural log units for  $T \leq 1$  s, and 0.46 to 0.91 natural log units for  $T > 1$  s.

Table 3 Central, high, and low estimates of sigma for the two simulation approaches

	Physic-Based			Stochastic		
	Central	High	Low	Central	High	Low
$T \leq 1$ s	0.59	0.74	0.45	0.69	0.83	0.56
$T > 1$ s	0.62	0.78	0.46	0.73	0.91	0.57

## 6. CONCLUSIONS

We used two different simulation approaches, a deterministic physics-based approach and a stochastic site-based approach, to model earthquake ground motions for large magnitude events in the CEUS. In general, the simulated ground motions are in agreement with the available CEUS GMPEs. At most periods and distances, the medians of the simulated ground motions are centered within the range of values predicted by the 17 GMPEs of the NGA-East for the USGS model and are close to the 2014 USGS GMPE combination in terms of amplitude and attenuation with distance. The variability of the simulated ground motions are evaluated, and the variation of sigma with distance, period, and magnitude are discussed. The synthetic sigmas are comparable to the estimates from the GMPEs used in the 2014 USGS model and from the NGA-East for the USGS model. Based on our simulations and comparisons with available

GMPEs, we recommend a sigma range for the CEUS, which is 0.45-0.83 natural log units for  $T < 1$  s, and 0.46-0.91 natural log units for  $T > 1$  s.

## 7. REFERENCES

- Al Atik L. (2015). NGA-East: Ground motion standard deviation models for Central and Eastern North America, PEER Report No. 2015/09, Pacific Earthquake Engineering Research Center, University of California, Berkeley, CA.
- Atkinson, G. M., and D. M. Boore (2006), Earthquake ground-motion prediction equations for Eastern North America. *Bull. Seismol. Soc. Am.* 96(6): 2181–2205
- Campbell K.W. (2003). Prediction of strong ground motion using the hybrid empirical method and its use in the development of ground motion (attenuation) relations in Eastern North America, *Bull. Seismol. Soc. Am.*, 93:1012–1033
- Crempien, J., and R. Archuleta (2017). Within-event and between-events ground motion variability from earthquake rupture scenarios. *Pure Appl. Geophys.*, 2017, 174 (3),1-15.
- D’Amico M., Mara Monica Tiberti, Emiliano Russo, Francesca Pacor, and Roberto Basili (2017). Ground-motion variability for single site and single source through deterministic stochastic method simulations: Implications for PSHA. *Bull. Seismol. Soc. Am*, Vol. 107, No. 2, pp. 966–983
- Frankel, A., E. Wirth, N. Marafi, J. Vidale, and W. Stephenson (2018). Broadband synthetic seismograms for magnitude 9 earthquakes on the Cascadia megathrust based on 3D simulations and stochastic synthetics: Methodology and overall results, *Bull. Seismo. Soc. Am.*, doi: 10.1785/0120180034.
- Goulet, C. A., Y. Bozorgnia, N. Kuehn, L. Al Atik, R. R. Youngs, R. W. Graves, and G. M. Atkinson (2017). NGA-East ground-motion models for the U.S. Geological Survey national seismic hazard maps, Pacific Earthquake Engineering Research Report No. 2017/03, Berkeley, CA.
- Hartzell, S., M. Guatteri, P. Martin Mai, P.-C. Liu, and M. Fisk (2005). Calculation of broadband time-series of ground motion, part II: Kinematic and dynamic modeling using theoretical Green’s functions and comparison with the 1994 Northridge earthquake, *Bull. Seism. Soc. Am.*, 95, 614-645.
- Imtiaz, A., M. Causse, E. Chaljub, and F. Cotton (2015). Is ground-motion variability distance dependent? Insight from finite-source rupture simulations, *Bull. Seismol. Soc. Am.*, 105 (2A), 950–962.
- Keefer D.L., Bodily S.E. (1983). Three-point approximations for continuous random variables, *Management Sci.*, 29: 595–609.
- Moschetti, M., S. Hartzell, L. Ramírez-Guzmán, A. Frankel, S. Angster, and W. Stephenson (2017). 3D ground-motion simulations of Mw 7 earthquakes on the Salt Lake City segment of the Wasatch Fault Zone: Variability of long-period ( $T \geq 1$ s) ground motions and sensitivity to kinematic rupture parameters, *Bull. Seismol. Soc. Am.*, 107 (4), 1704-1723.
- Petersen, M. D., M. P. Moschetti, P. M. Powers, C. S. Mueller, K. M. Haller, A. D. Frankel, Y. Zeng, S. Rezaeian, S. C. Harmsen, O. S. Boyd, N. Field, R. Chen, K. S. Rukstales, N. Luco, R. L. Wheeler, R. A. Williams, and A. H. Olsen (2014). Documentation for the 2014 update of the United States National Seismic Hazard Maps, U.S. Geol. Surv. Open-File Rept. 2014-1091, 242 p.
- Pezeshk S., Zandieh A., Tavakoli B. (2011). Hybrid empirical ground-motion prediction equations for Eastern North America using NGA models and updated seismological parameters, *Bull. Seismol. Soc. Am.*, 101(4), 1859–1870.
- Rezaeian, S., and A. Der Kiureghian (2010). Simulation of synthetic ground motions for specified earthquake and site characteristics, *Earthq. Eng. Struct. Dynam.*, 39, 1155-1180.
- Rezaeian, S., S. Hartzell, X. Sun, and C. Mendoza (2017). Simulation of earthquake ground motions in the eastern United States using deterministic physics-based and site-based stochastic approaches, *Bull. Seismol. Soc. Am.*, 107, 149-168.
- Saikia, C. K. (1994). Modified frequency-wavenumber algorithm for regional seismograms using Filon’s quadrature: Modeling of  $L_g$  waves in eastern North America, *Geophys. J. Int.*, 118, 142-158.
- Silva W.J., Gregor N., Darragh R. (2002). Development of regional hard rock attenuation relations for Central and Eastern North America, Technical Report, Pacific Engineering and Analysis, El Cerrito, CA.
- Sun, X., S. Hartzell, and S. Rezaeian (2015). Ground-motion simulation for the 23 August 2011, Mineral, Virginia, earthquake using physics-based and stochastic broadband methods, *Bull. Seism. Soc. Am.*, 105, 2641-2661.
- Sun, X., B. Clayton, S. Hartzell, and S. Rezaeian (2018). Estimation of ground-motion variability in the central and eastern united states using deterministic physics-based synthetics, *Bull. Seism.Soc. Am.*, doi: 10.1785/0120180030
- Tavakoli, B., Pezeshk, S. (2005). Empirical-stochastic ground-motion prediction for Eastern North America. *Bull. Seismol. Soc. Am.*, 95(6), 2283–2296
- Vyas J. C., Paul Martin Mai, and Martin Galis (2016). Distance and azimuthal dependence of ground-motion variability for unilateral strike-slip ruptures. *Bull. Seism.Soc. Am.*, 106 (4), 1584–1599.